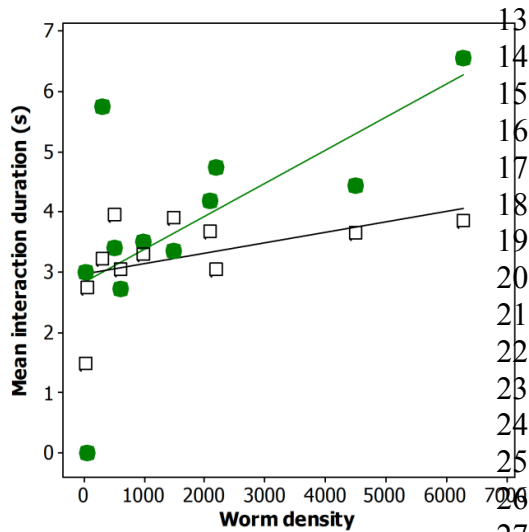


4 **Additional information about the statistical analysis**

5 **Figure 1. (c)** Initially we fitted a linear regression model with an intercept which  
 6 showed a significant relationship between number of interactions per frame in the  
 7 experimental videos and the null model simulations for the same values of worm  
 8 density (slope = 1.206,  $t_9 = 9.79$ ,  $p < 0.001$ ,  $R^2 = 91.4\%$ ) and fitted the data well (the  
 9 residuals were compatible with a Normal distribution, Anderson-Darling test: AD =  
 10 0.334,  $n = 11$ ,  $p = 0.440$ ). However, the intercept was not significantly different from  
 11 zero (intercept = -0.018,  $t_9 = -0.01$ ,  $p = 0.992$ ). Given this and the absence of  
 12 interaction at 0 density, we fitted a new linear regression model through the origin.



13 **Figure 1. (d)** “Worm density” is calculated  
 14 as  $L^2 n (n-1)$  where  $L$  is the mean length of  
 15 the worms and  $n$  is the number of worms  
 16 in the arena. Hence, this measures the  
 17 total length of worms in a sample and yet  
 18 accounts for individual worms not crossing  
 19 themselves. Initially we fitted a General  
 20 Linear Model (GLM) to the mean duration  
 21 of polarization interactions with predictors  
 22 treatment (experimental videos or null  
 23 model simulations) as a fixed factor and  
 24 worm density as a covariate. There was a  
 25 significant relationship between mean  
 26 interaction duration (s) and worm density  
 27 ( $F_{1,18} = 8.70$ ,  $p = 0.009$ ) but treatment ( $F_{1,18} =$

28  $= 0.04$ ,  $p = 0.845$ ) and the interaction between treatment and worm density ( $F_{1,18} =$   
 29  $2.34$ ,  $p = 0.144$ ) did not have significant effects. The model did not fit the data well  
 30 ( $R^2(\text{adj}) = 30.69\%$ ) and the residuals were not compatible with a Normal distribution  
 31 (Anderson-Darling test: AD = 1.228,  $n = 22$ ,  $p < 0.005$ ). A  $\log_{10}$  transformation of the  
 32 response variable gave the same qualitative results but this time  $R^2(\text{adj}) = 32.54\%$   
 33 and the residuals were compatible with a Normal distribution (Anderson-Darling test:  
 34 AD = 0.548,  $n = 22$ ,  $p < 0.140$ ). We can conclude that a reduced model with worm  
 35 density as the only predictor is the best model and hence there is no evidence to  
 36 suggest that either the intercepts or slopes for this relationship are different between  
 37 the experimental videos and the null model simulations. However, while the gradient  
 38 of the relationship between  $\log_{10}$  mean interaction duration (s) and worm density is  
 39 significantly different from 0 for the videos, this is not the case for the null model  
 40 simulations (figure 1d). This means that the relationship between interaction duration  
 41 and density is entirely attributable to the videos. Note that the  $\log_{10}$ -transformation in  
 42 figure 1d excludes the videos point with mean interaction duration of 0s at 0 worm  
 43 density, which, if included, as in the plot above, has a lot of leverage, even though  
 44 the results remain qualitative the same.

45

46

47 **Figure 1. (e)** The residuals were nearly-normal (Anderson-Darling test: AD = 0.958,  
 48 n = 14, p = 0.011). The slope of 0.85779 had a s.e. = 0.02215. The critical t-value at  
 49 d.f. = 12 and alpha = 0.05 (two-tailed) is 2.179. Therefore, the 95% CI for the  
 50 gradient is (0.80953, 0.90605). The critical t-value at d.f. = 12 and alpha = 0.001 (two-  
 51 tailed) is 3.055. Therefore, the 99% CI for the gradient is (0.79012, 0.92546).

52 **Figure 2. (b)** The model fits the data well (Hosmer-Lemeshow goodness-of-fit test:  
 53  $\chi^2 = 14.83$ , n = 8, p = 0.062) and has good predictive power (concordance = 95.5%;  
 54 Somers' D = 0.91). It was fitted after the removal of four outliers (1 for milling and 3  
 55 for no milling; n = 81, 27 milling and 54 no milling) identified from the delta beta, delta  
 56 deviance and delta chi-square residual plots. The predicted probabilities for these  
 57 points did not fit the observed outcome well. However, the model fitted to all the 85  
 58 data points gave the same qualitative results, namely that with every additional worm  
 59 per ml the probability of milling increases on average by 2% (95% CI: 1 – 3%).

60 **Figure 3. (c)** The initial binary logistic regression model had proportion milling as the  
 61 response variable and density, bias (rad) and the interaction between the two as the  
 62 predictors but bias (chi-sq = 2.335, d.f. = 4, p = 0.674) and the interaction (chi-sq =  
 63 1.646, d.f. = 4, p = 0.801) did not have a significant effect. The model was refitted  
 64 without the interaction. Now both density (coefficient = 0.0710, p < 0.001) and bias  
 65 (chi-sq = 58.413, d.f. = 4, p < 0.001) had significant effects. This model had a good fit  
 66 (all goodness-of-fit tests had a p-value > 0.05, except Brown's tests for an alternative  
 67 link function with 0.01 < p-value < 0.05) and excellent predictive power (Somers' D =  
 68 0.96). For differences between inflection points for different levels of bias, please see  
 69 table S1.

70 **Supplementary tables and figures**

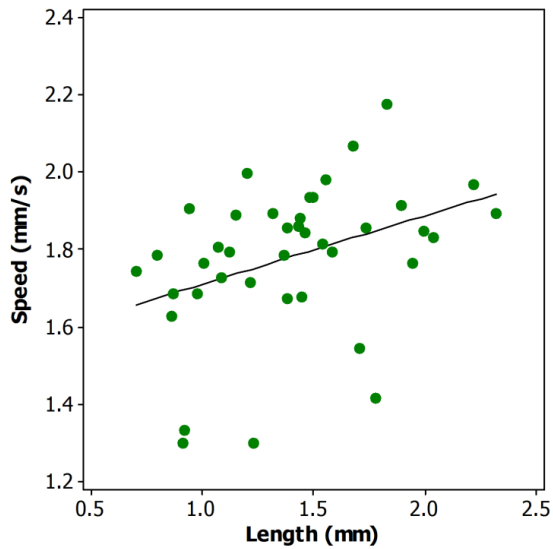
71 **Table S1.** Differences between inflection points for different levels of bias (rad) in the  
 72 movement of individual worms in the simulation of interacting worms (figure 3c).

<b>Bias (rad)</b>	<b>-0.13</b>	<b>-0.06</b>	<b>0.00</b>	<b>0.06</b>	<b>0.13</b>
<b>-0.13</b>	180	Z = -4.98 p < 0.001	Z = -7.05 p < 0.001	Z = -4.81 p < 0.001	Z = -0.94 p = 0.345
<b>-0.06</b>		228	Z = -3.86 p < 0.001	Z = 0.26 p = 0.798	Z = 4.34 p < 0.001
<b>0.00</b>			256	Z = 4.06 p < 0.001	Z = 6.69 p < 0.001
<b>0.06</b>				226	Z = 4.15 p < 0.001
<b>0.13</b>					189

73 0.00 rad represents no bias; both -0.06 and 0.06 rad, and -0.13 and 0.13 rad  
 74 represent equal levels of bias clockwise and anticlockwise, respectively; numbers  
 75 along the diagonal represent inflection point densities (i.e. the number of worms per  
 76 simulation arena); z-values and p-values represent differences between the inflection  
 77 points as measured by differences between the constants in the binary logistic  
 78 equation for different levels of bias (since the inflection point is equal to the constant  
 79 divided by the coefficient for density, which is the same for all levels of bias)

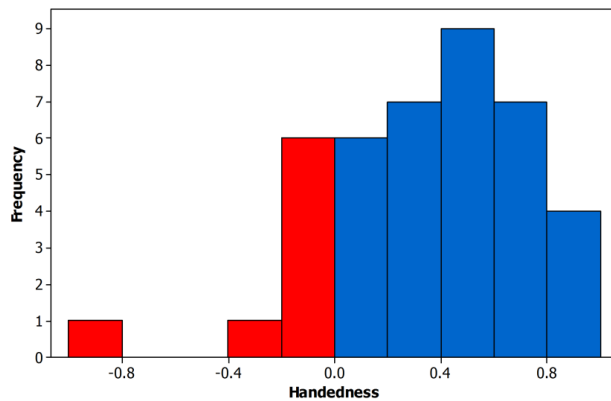
80  
 81

82



83

84 **Figure S1.** The relationship between mean speed and body length is best described  
85 by the line: worm speed ( $\text{mm}\cdot\text{s}^{-1}$ ) =  $1.53 + 0.178$  worm length (mm). ( $F_{1,38} = 6.13$ ,  $p =$   
86  $0.018$ ,  $R^2 = 0.139$ ). The average mean speed of these 40 worms was  $1.78 \text{ mm}\cdot\text{s}^{-1}$ .  
87 One worm, which was much smaller than the rest (just over 0.5 mm long) was  
88 removed from this analysis. With this individual, the mean speed was  $1.76 \text{ mm}\cdot\text{s}^{-1}$ .

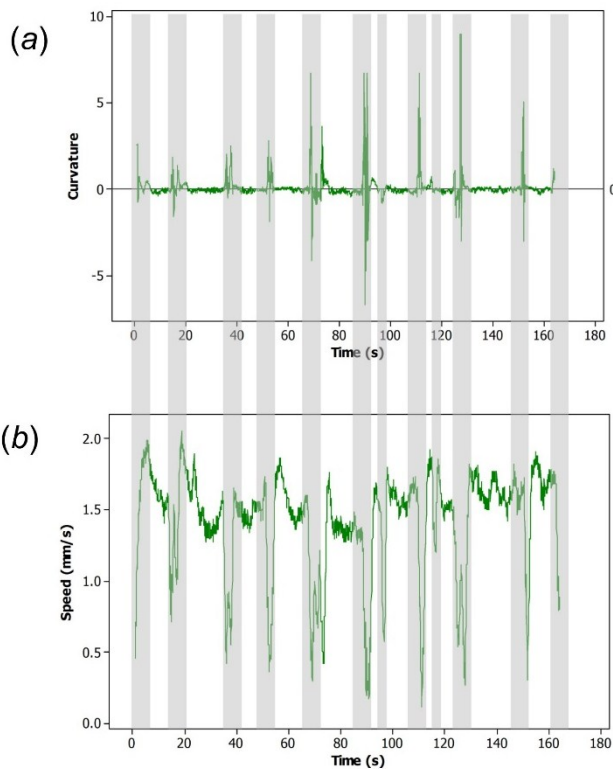


89

90 **Figure S2.** Turn direction for 41 worms as summarised by a handedness variable  $h$   
91 =  $(C-A)/(C+A+S)$  where C, A and S are the numbers of clockwise, anticlockwise and  
92 straight-on manoeuvres respectively. The worms are predominantly right biased –  
93 making clockwise movements; blue: right-biased or clockwise movement, red: left-  
94 biased or anticlockwise movement.

95

96



98

99

100

101

102

103

104

105

**Figure S3.** Worms executing curved trajectories are slower. (a) A worm's body curvature over time and (b) the speed of the same worm over the same 165s. Comparison of (a) and (b) shows that when the worm curves its body its speed dips as indicated by the grey bars. The even spacing of the grey bars suggests some rhythmicity to the changes in body curvature and speed (see also figure 1a). The curvature  $c$  is the reciprocal of the radius of curvature multiplied by  $\pm 1$  depending upon whether the turning direction is clockwise or anticlockwise.

106

107

```

108 Place N worms at random in the arena - each worm consists of two rigid rods of equal length
109 L units with a random angle in the range +/-0.05 radian between them.
110 For as many iterations as required, each representing dt seconds of real time
111 begin
112   Scramble the order of the worms
113   For each worm in turn
114     begin
115       Determine the centre of the circumcircle defined by the head, centre and tail positions
116       Determine the curvature of this circle = 1.0/radius of curvature
117       Calculate the worm speed = nominal speed*(1.0 - g*curvature)
118       Calculate  $d\theta$  = speed*curvature*dt = the angle that the worm advances inside its
119         circumcircle
120       Calculate the new x,y coordinates of the worm tail, centre and head
121       For four alternative head positions
122         begin
123           Calculate alternative head positions with angles within +/-0.15 radian of the initial
124             one
125         end
126       For the total of five head positions
127         begin
128           Set the potential energy to zero
129           For all other worms within the distance  $r_{max}$ 
130             begin
131               Calculate the distance between the chosen head position and the tail of its
132                 neighbour
133               Add the energy as determined from the potential energy curve (figure 3a)
134               Calculate the distance between the chosen head position and the head of its
135                 neighbour
136               Calculate the potential energy using figure 3a
137               If the tails of the two worms are separated by  $>2L$ , set  $\lambda=0.5$ , else  $\lambda=2.0$ 
138               Add the energy multiplied by the weighting factor  $\lambda$ 
139             end (loop over worm's near neighbours)
140           end (loop over possible head positions)
141           Adopt the head position with the lowest total energy
142           If the head is outside the arena, re-orient wholly within the boundary and facing inwards
143         end (loop over the N worms)
144       end (iteration loop)
145
146 L = 5 units (length of each of the two rods making up a worm)
147 V = 11.07 s-1 (nominal speed in units.s-1 – real worms move their own length in ~1s)
148 dt = 0.7s (elapsed time per iteration)
149 g = 2.98 (speed reduction coefficient)
150 r – range of interaction
151  $r_{max}$  = 25 units (the maximum range of any interaction – see figure 3a)
152  $r_{min}$  = 5 units (the range at which attraction is at its maximum – see figure 3a)

```

153 **Figure S4.** Pseudocode for the simulation with interacting worms.

154

155

156

1. Are circular mills more likely to form near the arena walls?

(a)	0	4	17	(b)	3	5	2
	0	8	2		5	9	5
	7	4	3		7	4	5

157

158

159

160

161

(a) For the data collected in 2015, the positions of a total of 45 occurrences of circular mills were recorded on a 3x3 grid in 30 arenas of different shapes and sizes.

(b) For the simulation of interacting worms, the formation positions of circular mills were recorded on a 3x3 grid for a total of 45 runs.

162

163

164

165

166

167

168

169

170

171

172

173

We compared a null model based on the assumption that a circular mill is equally likely to occur in any of the 9 cells of the 3x3 grid with (a) data on real worms and (b) data from the simulation of interacting worms. On the basis of the null model and the 45 circular mills observed altogether in the data for real worms, the probability of a cell containing no more than 1 circular mill is less than 5% and the probability of a cell containing no less than 10 circular mills is less than 5%. Therefore, for the data, the 17 circular mills observed in the top right cell are significantly more than expected by chance and the zero circular mills observed in the top and middle left cells are significantly fewer than expected by chance. The former could be explained by the orientation of the top right cell towards the sun. For the simulation with interacting worms, the number of circular mills in each of the 9 cells was compatible with random expectation. We conclude, that circular mills are not more likely to form near the arena walls.

174

175

2. Does the shape of the arena (perimeter-to-area ratio) influence the formation of circular mills?

176

177

178

179

180

181

182

183

184

185

186

187

188

189

190

191

192

193

194

195

196

197

We tested this in the simulation with interacting worms by comparing the formation of circular mills in two arenas with the same areas but with different shapes: one was circular (radius = 400 units), the other was square (with a side of  $2\sqrt{354.49}$  units). Therefore, although the two arenas had the same area, the perimeter of the square was 1.1284 times greater. Each arena had the same number of worms ( $n = 1016$ ) and hence the same density. Hence, any difference between the formation of circular mills in the two arenas could be attributed to the difference in their shapes. We let the program run, repeatedly, for a fixed amount of (worm) time and at the end checked whether there was a mill or not. Every run that produced a mill at the end was counted as a success. No credit was given for a mill that formed before the end and then dispersed, nor for pairs of mills that merged. And if there were two at the end, it simply counted as a success. The initial worm time was 4min 30s. It was chosen on the basis of an approximately 50% success rate and was also long enough to allow any worm to cross either arena about three times. (The arenas were both ~800 units across and the worms 10 units long. Real worms cover their own length in ~1s so our simulated worms needed about 80s to cross the arena, so 4m 30s is ~3 crossings). The results from 1500 runs on each arena were: 839 successes for the circle and 577 successes for the square. We extended the time for each run to 10min to test whether this would narrow the difference in the success rate between the two arena shapes. If the production of mills in 100% of the runs is a matter of waiting long enough, that would suggest that the longer perimeter only delays the formation of circular mills. Indeed, the results from 500 runs of 10min duration on each arena resulted in 461 successes in the circle and 449 success in the square. We conclude that a longer perimeter of the arena delays the formation of circular mills.

198

199

Overall, our results suggest that, if anything, circular mills are more likely to form near the centre.

200

**Figure S5.** Analysis of the role of the arena walls in the formation of circular mills